Article

JOURNAL OF COMPOSITE MATERIALS

Journal of Composite Materials
47(1) 27–32

DOI: 10.1177/0021998312459779
jcm.sagepub.com

SAGE

Design of dye-sensitized solar cells integrated in composite panel subjected to bending

Morio Nagata[1], Eli Baldwin[2], Sooyeun Kim[3] and Minoru Taya[3]

Abstract

This article discusses the design of airborne dye-sensitized solar cell (DSSC) panel integrated in the airplane composite panel which is subjected to mechanical dynamic loading so that the DSSC will function continuously as airborne energy harvester. This article consists of two parts, first synthesis of more rubut DSSC, and then its integration into a composite panel with durability demonstrated.

Keywords

DSSC, integration, durability, solar energy harvester, bending, UAV

Introduction

Unmanned air vehicles (UAVs) are driven by ordinary engines such as gasoline engine, thus, its flight time is limited by the capacity of the fuel tank which contains gasoline. In order to increase UAV flight time, use of energy-harvesting unit from environment is desirable. Among many energy-harvesting schemes, solar cells seem to be most logical as a UAV flies in the sky where solar energy is abundant, particularly at higher altitudes. Even in cloudy weather, dye-sensitized solar cells (DSSC) have some advantages over Si-based solar cells or other more expensive but higher performance semiconductor based solar cells, i.e., at a lower cost, DSSC work better than Si-solar cells in cloudy conditions. However, the integration of solar cells to airborne structures has not been well studied. The NRL group headed by Thomas [1,2] has studied the feasibility of using solar cells in small UAVs, and concluded that in order to power a UAV by solar cells only, one needs to use the solar cells of higher power conversion efficiency (PCE). PCE value of typical DSSC is 6–10%, but use of such DSSCs in a UAV or micro-air vehicle (MAV), seems to be still justifiable to increase flight time as well as powering additional sensors and actuators mounted in such a UAV and MAV. Then, an ideal UAV propulsion system would be driven by the electric motor connected to propeller, which is powered by the solar energy harvesting system mounted on the UAV structures including wings. For such solar energy harvesting systems, low-cost DSSCs are better suited.

The first successful DSSC design was made by the Osaka University group [3,4] who used porous ZnO with rose Bengal dye dipped in the electrolyte solution of KI-I2. This DSSC exhibited the power conversion efficiency of 1.5% and quantum yield of 15% and open voltage of 0.38 V. The above design has two unique features, use of porous semiconductor, ZnO and electrolyte of KI-I2. The former contributed to the effective adsorbance of dye on the porous surface of ZnO and the latter makes the DSSC electrochemically stable. They also studied the photocurrent dependence on several parameters, concentration of dye in solution [4] and pH of the solution and use of other metal oxides such as TiO_2 [5]). The above pioneered DSSC design was much improved by O'Regan and Grätzel [6] who used nanostructured TiO_2 and a new dye based on

[1]University of Tokyo, Research Center for Advanced Science, Tokyo, Japan
[2]The Boeing Commercial Company, Seattle, WA, USA
[3]Center for Intelligent Materials and Systems, Department of Mechanical Engineering, University of Washington, Seattle, WA, USA

Corresponding author:
Minoru Taya, Center for Intelligent Materials and Systems, Department of Mechanical Engineering, University of Washington, Box 352600, Seattle, WA 98195, USA.
Email: tayam@u.washington.edu

rutenium complex where nanostructured TiO_2 layer of 10 μm thickness (the average size of single particles is 12 nm) was used. The DSSC exhibited the open circuit voltage of 0.78 V and short circuit current of 1.3 mA/cm^2. This DSSC with size 5 mm^2 showed the power conversions efficiency (PCE) of 7.9% under AM1.5 sun light condition and 12% PCE under diffuse light condition. The fill factor of the DSSC under low intensity sun light condition (5 W/m^2) is 0.7. This is higher than that of conventional silicon based photovoltaic, which is less than 0.5. This means that use of DSSC in dim light conditions (morning and late afternoon sun lights, cloudy days and inside building) is more advantageous than the conventional silicon based solar cells. They performed limited durability test on the DSSC, 2 months under visible lights ($\lambda > 400$ nm), resulting in only 10% reduction in the photocurrent.

Since the above pioneering works, many research groups are working on DSSC with aim of improving higher PCE [7], and larger sized DSSC [8], flexible DSSC [9] and using dye which can absorb light of longer wavelengths including near IR waves [10]. One can refer to a recent review paper on DSSC development [11]. The basic principle of DSSC is illustrated in Figure 1 where (a) shows the nanostructure design and (b) the electron flow. Once the dye absorbs sun light, it is excited and there is an increase in its energy level higher than that of TiO_2, thus converting photons to electrons. These are passed to TiO_2, then to the working electrode, and further on to the electric current circulating the electric wire, reaching the counter electrode, i.e., the electrons come to the counter electrode, pass through iodine which is now reduced, and thus, holes are emitted from the dye to complete the redox cycle.

In order to design a DSSC system to be integrated in the wing structures of a UAV, a MAV or a manned air vehicle, several requirements need to be satisfied, and they are: (i) the integrated DSSC needs to be durable for a longer time under usage environment, such as under dynamic bending loading condition, (ii) the electrolyte must perform well even in lower temperatures, which are required for flying at higher altitudes. This article is aimed at designing such airborne integrated DSSC systems by using thin glass substrate (0.3 mm thick) and also lower-temperature resistant electrolyte (up to −50°C).

Experimental

Materials and reagents

Iodine, 4-tert butyl-pyridine (TBP), tetrabutylammonium iodide (TBAI), poly(vinylidenefluoride-co-hexafluoropropylene) (P(VDF-HFP)), 3-methoxypropionitrile (MPN), acetonitrile, tert-butyl alcohol, ethanol and chenodeoxycholic acid (Cheno) were purchased from Sigma-Aldrich. Methyl-3-n-propyl-imidazolium iodide (MPImI) was purchased from TCI America. Transparent conducting oxide glass substrates (Fluorine doped SnO_2 layer with sheet resistance of 3.5 ohm/sq, NEG, Japan) were washed under ultra-sonication for 10 min with neutral detergent, DI water, ethanol, respectively, followed by UVO cleaning (Jelight Company, Inc) for 10 min before use. Commercial TiO_2 (Ti-Nanoxide T and D, Solaronix SA, Switzerland) was used for the preparation of the nanocrystalline films. Pt catalyst (T/SP, Solaronix SA, Switzerland) was used for the preparation of the counter electrode.

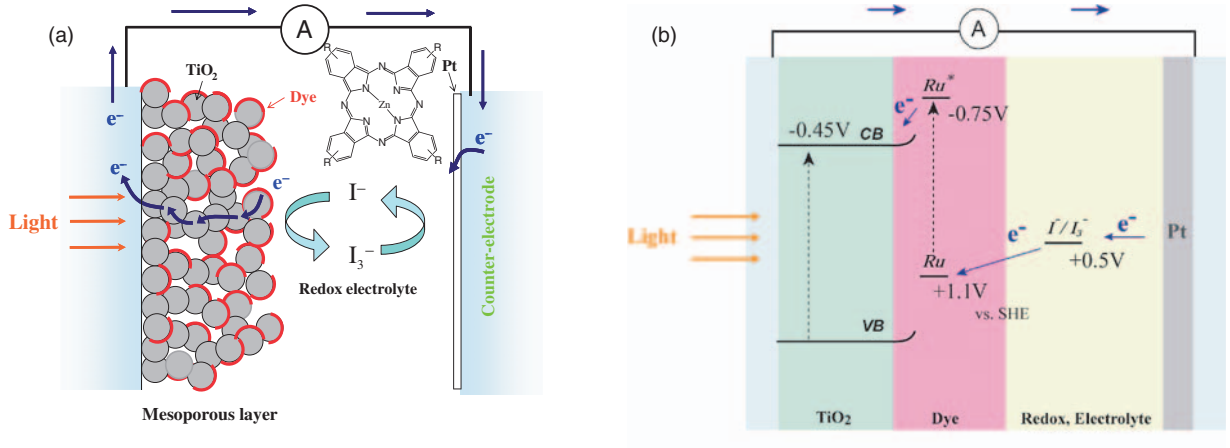

Figure 1. Working principle of a DSSC: (a) nanostructure made of the working electrode of transparent electrode (FTO), TiO_2 layer with dye, electrolyte of iodine and counter electrode of Pt, (b) flow chart of electrons within the frame work of band gap of TiO_2, dye and redox potential of iodine electrolyte.

Table 1. Three different gel electrolytes used in this study

Type of gel electrolyte	Ingredients
A	0.12 M I_2, 0.2 M TBP, 5 wt% P(VDF-HFP), 0.8 M MPIml in 3-Methoxypropionitrile
B	0.12 M I_2, 0.2 M TBP, 5 wt% P(VDF-HFP), 0.8 M TBAI in 3-Methoxypropionitrile
C	0.12 M I_2, 0.2 M TBP, 5 wt% P(VDF-HFP), 0.7 M MPIml, 0.1 M TBAI in 3-Methoxypropionitrile

Preparation of gel electrolytes

We use three different gel electrolytes, A, B and C, whose ingredients are given in Table 1. The solution was stirred until all chemicals were completely dissolved. 5 wt% P(VDF-HFP) was dissolved in the solution at 90°C. After cooling down to room temperature, the gel electrolyte was formed.

Preparation of dye-adsorbed TiO_2 films

The doctor blade method was used to fabricate TiO_2 films on FTO glass (thickness of 0.3 mm, Nippon Electric Glass company). The electrode coated with the TiO_2 paste (Ti-Nanoxide T and D, Solaronix SA) was shortly dried in air at 100°C, followed by sintering at 500°C for 30 min. A TiO_2 film of 12 μm thickness was used as the working electrode on which dye is mounted. After sintering, it cooled down to 70°C. The TiO_2 electrode was immersed in the solution (acetonitrile:tert-butyl alcohol = 1:1) with 0.5 mM cis-dithio-cyanate-N,N'-bis-(4-carboxylate-4-tetrabutylammonium carboxylate-2,2′-bipyridine) ruthenium(II) (N719) and kept at room temperature for 12 h. The dye-coated electrodes were rinsed quickly with ethanol.

Fabrication of dye-sensitized solar cells

The electrochemical cell used for photovoltaic measurements consisted of a dye-adsorbed TiO_2 electrode, a Pt-coated counter electrode, a spacer, and an organic electrolyte. The FTO glass was drilled to make two tiny holes. Pt catalyst (Pt-Catalyst T/SP, Solaronix SA) was deposited on the FTO glass by using the doctor blade method and treated at 400°C for 30 min. The two electrodes were sandwiched with the spacer. The 25 μm thick hot-melt film (Surlyn, Solaronix) was used as a spacer. It was heated at 120°C for 2 min. The electrolyte was introduced into the cell by using a pipette. Two holes were sealed with UV adhesive (31X-101B, ThreeBond) and a thin glass.

Photovoltaic characterization

The photoelectrochemical performance of the solar cell was measured using OTENTO-SUN II (Bunkoh-Keiki Co., Ltd., Japan). A 500-W Xe lamp served as the light source in combination with a band-pass filter (400-800 nm) to remove ultraviolet and infrared radiation and to give 100 mW cm^{-2} (the equivalent of one sun at AM 1.5) at the surface of the test cell. The incident light intensity was calibrated by a standard Si solar cell (BS-520, Bunkoh-Keiki Co., Ltd., Japan) and solar tester (SCR-200, Bunkoh-Keiki Co., Ltd., Japan). UV-vis. absorption spectra were recorded with a JASCO model V-570 spectrophotometer.

Integration and bending tests

Integration of a DSSC of size (5 mm × 5 mm) into a polymeric composite panel (woven composite panel of length 142 mm, width 29.3 mm and thickness 1.52 mm) is made by bonding only the end area of the PET film to the composite panel, see Figure 2(b). As a comparison, we also made another integration of bonding directly DSSC to the composite panel, see Figure 2(a). The polymer adhesive used for the above bonding is 3 M Scotch Weld AF-163, curing condition 120 min at 80°C.

The bending test for the integrated DSSC to composite panel was performed by placing the composite panel under four-point bending jig as shown in Figure 3. In this figure, the DSSC is mounted at the bottom of the composite beam, four-point load span is 48 mm and the support span is 100 mm.

The composite panel used for the bending test is woven composite and its dimensions are length of 110 mm, width of 29.3 mm and thickness of 1.52 mm, and its longitudinal Young's modulus is 18.5 GPa.

We performed two sets of bending tests: (i) static bending test (both under tension and compression) to measure the failure bending strain at which the adhesive site is broken, or debonding of the working and counter electrodes of the DSSC and (ii) cyclic bending test to measure residual PCE of the DSSC under zero to tensile bending strain condition with cyclic frequency of 2 Hz. Range of applied radius of curvatures (R) being 15–50 cm, where the corresponding bending strain at the DSSC site to $R = 15$ cm is 0.1% and that to $R = 50$ cm is 0.03%, respectively. It is noted that the bending strain at the surface of the composite (ε_b) is given by

$$\varepsilon_b = h/(2R) \quad (1)$$

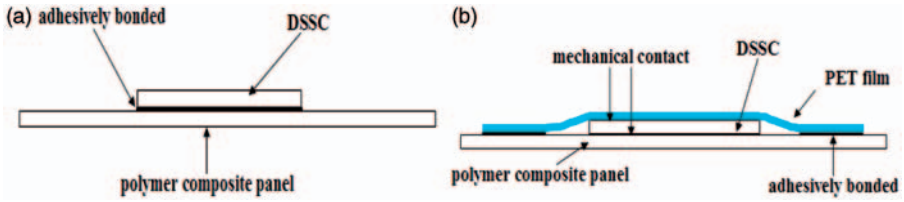

Figure 2. Two bonding designs of a DSSC to a composite panel: (a) bonding condition 1: direct bonding to the composite panel by polymer adhesive, (b) bonding condition 2: PET film covering a DSSC with mechanical touch while the ends of the PET bonded adhesively.

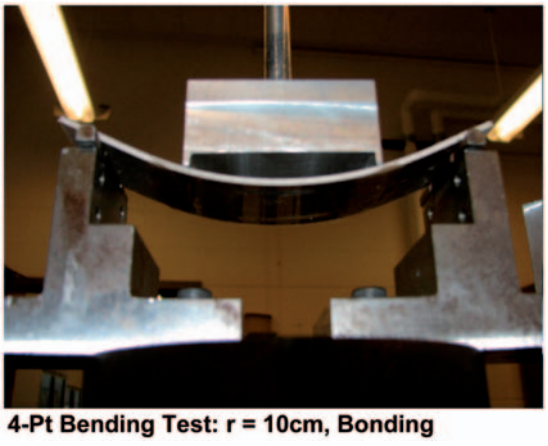

Figure 3. Four point bending test for integrated DSSC to composite beam where the DSSC is mounted at the bottom of the beam.

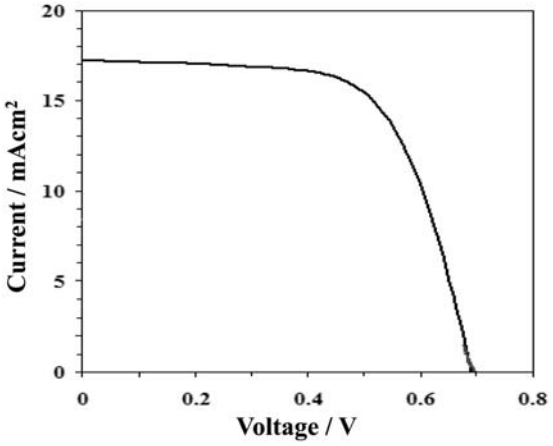

Figure 4. Current-voltage characteristics for DSSC of 4 mm × 6 mm size based on gel electrolyte C and N719 dye, providing PCE = 7.8%.

where h is the thickness of the composite plate and R is the radius of curvature. It is noted that the exact bending strain imposed on the top(working electrode) and bottom side (counter electrode) of the DSSC are slightly larger due to the locations there are larger than $h/2$. But for the purpose of recording of our bending strain, we used equation (1).

Results and discussion

N719 dye based DSSC

Iodine based electrolytes can be optimized in terms of efficiency and stability. Better stability can be obtained by modifying the TiO_2-dye interface and reducing the vapor pressure of the electrolyte's solvent. The latter is especially important for outdoor applications where cyclic temperature changes require very robust sealing. Low-viscous solvents, liquid electrolytes may result in leakage of the cell. To avoid any leakage of the electrolyte, we use solidified (or gel) electrolytes which can be processed by polymerization of a precursor solution containing the monomer/oligomer and the iodide/iodine redox couple. The TiO_2-network is completely filled with the solid state electrolyte in the negligible vapor pressure. We optimized gel electrolytes for N719 dye based DSSC and investigated their stability. Figure 4 shows the I-V curves of DSSC based on gel electrolyte C and N719 dye. PCE was calculated as follows,

$$\mathrm{PCE}(\eta) = P_m/P_{in} \quad (2)$$

where P_m is volt × current at maximum power point and P_{in} is the power under the solar energy of 100 mW/cm^2 (AM 1.5 constant)

Electrolyte C (see Table 1) based DSSC exhibited the highest PCE of 7.8% in Figure 4. It also shows good stability over 50 days as demonstrated in Figure 5.

Resistance of DSSC against bending

A summary of the static bending tests applied to DSSC mounted on composite panel under bonding condition 1 (see Figure 2(a)) and condition 2 (Figure 2(b)) is given in Table 2 where the failure strains under tensile and

compressive bending stress loading are measured. The definition of failure is that either the DSSC bonding is detached, or the PCE of the DSSC is dramatically dropped from the starting value of PCE = 7.8%. The most common failure is observed in terms of detachment of the working or counter electrode of DSSC, thus, stop functioning of the energy harvesting, i.e., dropping of PCE value.

It is clear from Table 2 that the bonding condition 2 (Figure 2(b)) exhibits higher tolerance against bending due to its higher values of the failure bending strain of over 0.15%.

The results of cyclic bending tests of the integrated DSSC to composite panel with bonding condition 2 are summarized in Figure 6.

It follows from Figure 6 that the DSSC integration based on Figure 2(b) is durable design, where the DSSC is mounted on the composite panel under mechanical touch with the covering PET film which is bonded directly to the composite panel. This is reasonable in bonding condition 2 as the bending stress at the surface of the composite plate is not transferred to the DSSC, as the interface between them is just mechanical touch. Whereas, for the DSSC, integrated directly to the composite, it exhibited the debonding of the working and counter electrodes of the DSSC, leading to rapid decrease in the PCE value. Therefore, further study remains to be carried out on strengthening the bonding of the working and counter electrodes of the DSSC by using stronger adhesive bonding while satisfying the electrochemistry requirements of the DSSC cell structure.

Conclusion

Optimum integration scheme of DSSC into a composite panel is studied with the finding that the integration of DSSC directly on the composite by adhesive bonding is not durable while the integration of DSSC to the composite panel via covered PET film is much more durable under cyclic bending loading. Such integrated DSSC into airborne structural surfaces with the proposed scheme discussed in this paper is expected to increase flight time of a UAV/MAV. In addition, the UAV/MAV may need to fly even in dim light conditions, i.e. early morning and late afternoon hours, for which the power conversion efficiency of DSSCs is known to exceed that of the Si-based solar cells.

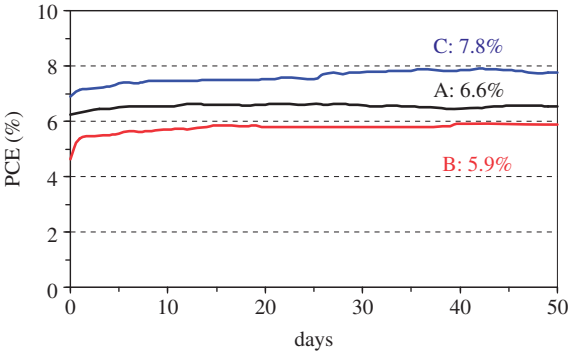

Figure 5. Stability of three different gel electrolytes (see Table 1) and N719 dye based DSSCs ($4 \times 6\,mm^2$) over 50 days.

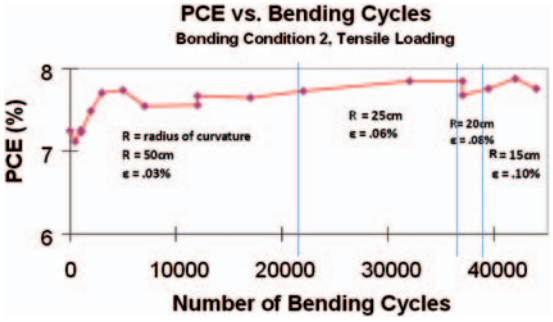

Figure 6. Power conversion efficiency (PCE) of DSSC integrated to composite panel subjected to bending strains (under zero and tensile) up to over 40,000 cycles with cyclic frequency 2 Hz where four different bending loading are used, radius of curvature (R) = 50 cm (bending strain = 0.03%), 25 cm (0.06%), 20 cm (0.08%) and 15 cm (0.1%).

Table 2. Failure bending strains of integrated DSSC to composite substrate under static bending tests where the bending strain has two modes, tension and compression (see Figure 3) and bonding conditions 1, and 2 are referred to Figure 2

		Failure strain (%ε)				
	Sample #	1	2	3	4	Average failure strain
Bonding condition 1	Tension	0.04%	0.10%	0.06%	0.04%	0.05%
	Compression	0.06%	0.04%	0.10%	0.15%	0.07%
Bonding condition 2	Tension	<0.15%	<0.15%	<0.15%	<0.15%	<0.15%
	Compression	<0.15%	<0.15%	<0.15%	<0.15%	<0.15%

Funding

This work was supported by a grant from AFOSR to University of Washington, under AFOSR-MURI on airborne energy-harvesting and storage systems (FA9550-06-1-0326) where Dr. Les Lee is the program manager and Taya is the Principle Investigator.

Acknowledgements

We are thankful to our researcher, Onur Cemal Namli, and former researcher, Rei Furukawa who helped a part of processing and testing of the present work.

References

1. Thomas JP and Qidwai MA. Mechanical design and performance of composite multifunctional materials. *Acta Mater* 2004; 52: 2155–2164.
2. Thomas JP, Qidwai MA, Baucom JN, Pogue WR. Multifunctional structure-power for electric unmanned systems *NATO AVT-141* (RTO-MP-IST-999). 2008; 1–14.
3. Tsubomura H, Matsumura M, Nomura Y and Amamiya T. Dye-sensitized zinc oxide:aqueous electrolyte:platinum photocell. *Nature* 1976; 261(5559): 402–403.
4. Matsumura M, Nomura Y and Tsubomura H. Dye-sensitization on the photocurrent at zinc oxide electrode in aqueous electrolyte solution. *Bull Chem Soc Japan* 1977; 50(10): 2533–2537.
5. Matsumura M, Matsudaira S, Tsubomura H, Takata M and Yanagida H. Dye sensitization and surface structures of semiconductor electrodes. *Ind Eng Chem Prod RD* 1980; 19: 415–421.
6. O'Regan B and Grätzel M. A low cost, high efficient solar cell based on dye-sensitized colloidal TiO_2 films. *Nature* 1991; 353: 737–740.
7. Ito S, Murakimi TN, Comte P, Liska P, Grätzel C, Nazeeruddin MK, et al. Fabrication of thin film dye sensitized solar cells with solar to electric power conversion efficiency over 10%. *Thin Solid Films* 2008; 516: 4613–4619.
8. Okada K, Matsui H, Kawashima T, Ezure T and Tanabe N. 100 mm × 100 mm large-sized dye sensitized solar cells. *J Photoch Photobio A* 2004; 164: 193–198.
9. Miyasaka T, Ikegami M and Kijitori Y. Photovoltaic performance of plastic dye-sensitized electrodes prepared by low-temperature binder-free coating of mesoscopic titania. *J Electrochem Soc* 2007; 154(5): A455–A461.
10. Mori S, Nagata M, Nakahata Y, Yasuta K, Goto R, Kimura M, et al. Enhancement of incident photo-to-current conversion efficiency for phthalocyanine-sensitized solar cells by 3D molecular structuralization. *J Am Chem Soc Comm* 2010; 132: 4054–4055.
11. Grätzel M. Review on dye-sensitized solar cells. *J Photoch Photobio C* 2003; 4: 145–153.